Transforming growth factor-β1 and soluble co-inhibitory immune checkpoints as putative drivers of immune suppression in advanced basal cell carcinoma

Mahlatse C.M. Kgokolo [1], Nonkululeko Z. Malinga [1], Helen C. Steel [2], Pieter W. A. Meyer [2,3], Teresa Smit [4], Ronald Anderson [2], Bernardo L. Rapoport [2,4]*

[1]*Department of Dermatology, School of Medicine, Faculty of Health Sciences, University of Pretoria and Steve Biko Academic Hospital, Pretoria, South Africa.*

[2]*Department of Immunology, School of Medicine, Faculty of Health Sciences, University of Pretoria, Pretoria, South Africa.*

[3]*Tshwane Academic Division of the National Health Laboratory Service, Pretoria, South Africa.*

[4]*The Medical Oncology Centre of Rosebank, Saxonwold, Johannesburg, South Africa.*

2023 ASCO® ANNUAL MEETING

Abstract ID: 9567

UNIVERSITEIT VAN PRETORIA
UNIVERSITY OF PRETORIA
YUNIBESITHI YA PRETORIA

The Medical Oncology Centre of Rosebank
Personalised Cancer Care

Background

- Basal cell carcinoma (BCC) is the most common malignancy, comprising about 75% of all cases of skin cancer, and the incidence is rising[1,2].
- BCC rarely metastasizes and the mortality rate is low; however, the disease is associated with substantial morbidity[3].
- The hedgehog intracellular signalling pathway regulates cell growth, and aberrant activation of this pathway leads to BCC development[3]. The hedgehog inhibitors vismodegib and sonidegib are currently approved for systemic therapy of BCC in Europe[3,4,5].
- Hedgehog-dependent tumors are characterized by increased infiltration or the presence of suppressive immune cells, such as M2-like tumor-associated macrophages (M2-TAMs), myeloid-derived suppressor cells (MDSCs), regulatory T (Treg) cells, and cancer-associated fibroblasts (CAF)[6-10].
- BCC is associated with increased numbers of regulatory cells (Tregs) and a CAF-induced immunosuppressive microenvironment[11-14].
- Checkpoint proteins are critical for maintaining self-tolerance and modulating the immune responses of effector cells in normal tissues to minimize tissue damage. These proteins also modulate the immune infiltrates in the tumor microenvironment (TME). Cancer cells exploit the up-regulation or down-regulation of these proteins to evade the anti-tumor immune response[15,16].
- Soluble forms of immune checkpoint molecules (ICMs) have recently been identified and can be measured in human plasma; however, their biological and clinical significance remains essentially unknown[17,18].
- Co-inhibitory immune checkpoint proteins are primarily involved in promoting inhibitory cell-cell interactions in adaptive immunity, especially tumor immunity.
- The soluble cell-free variants of these molecules are detectable in the circulation of cancer patients where they retain immunosuppressive activity.
- Little is known about the systemic levels of these soluble co-inhibitory immune checkpoints in patients with various subtypes of basal cell carcinoma (BCC), which is the most invasive and treatment-resistant type of this most commonly occurring malignancy.

Methods

- The study population consisted of a total of 40 South African patients (12F:28M; mean age ±SD: 69.1 ± 11.1 years) with advanced BCC attending the Dermatology Screening Clinic at Steve Biko Academic Hospital, Pretoria, South Africa.
- The results of the cohort were compared to those of a group of control participants (n=20)
- Ethics approval was granted by the Research Ethics Committee of the Faculty of Health Sciences, University of Pretoria. Informed consent was obtained from all patients and control participants.

Measurement of the soluble co-inhibitory and co-stimulatory immune checkpoint proteins

- A Human Immuno-Oncology Checkpoint Protein Panel (Milliplex® MAP Kit, Merck, KgaA, Darmstadt, Germany) was used to simultaneously determine the plasma concentrations of seven co-inhibitory sICPs, namely BTLA, CTLA-4, PD-1, PD-L1, PD-L2, LAG-3 and TIM-3; eight co-stimulatory sICPs, namely CD27, CD28, CD40, CD80, CD86, GITR, GITRL, and ICOS; and two dual-active sICPs, namely HVEM and TLR2. The methodology was followed as per the manufacturer's instructions and as described previously. The sICP levels were assayed using a Bio-Plex Suspension Array platform (Bio-Rad Laboratories Inc., Hercules, CA, USA). The Bio-Plex Manager software 6.0 was used for bead acquisition and analysis of median fluorescence intensity. The results are reported as picograms (pg)/mL plasma.

Measurement of arginase 1

- A Human ARG1 ELISA Kit (E-EL-H0497, Elabscience, Houston, TX, USA) was employed for measuring the levels of arginase 1 present in the stored plasma samples. The results are reported as picograms (pg)/mL plasma.

Measurement of fibroblast activation protein

- Fibroblast activation protein levels were determined in the stored plasma samples using a Human Circulating Cancer Biomarker Kit (Milliplex® MAP Kit, Merck, KgaA, Darmstadt, Germany). The methodology was followed as described above for the immune checkpoint proteins. The results are reported as pg/mL.

Measurement of Regulated upon Activation Normal T cell Expressed and Presumably Secreted (RANTES)

- Levels of RANTES present in the stored plasma samples were determined using a Human RANTES ELISA Kit (E-EL-H6006, Elabscience, Houston, TX, USA).

Measurement of transforming growth factor-beta1

- Prior to the analysis of the plasma samples for TGF-β1 concentrations, latent TGF-β1 was activated to the immunoreactive form by the addition of 40 µL 1 N hydrochloric acid (HCl) to 280 µL of plasma diluted 8-fold. Following 10 minutes of incubation at room temperature, the samples were neutralized by the addition of 40 µL 1.2 M sodium hydroxide (NaOH)/ 0.5 M HEPES [4-(2-hydroxyethyl)-1-piperazineethanesulfonic acid]. Samples were then immediately assayed for TGF-β1 levels using a Human TGF- beta1 ELISA Kit (E-EL-0162, Elabscience, Houston, TX, USA). The same methodology was followed as described above for the arginase 1 ELISA. Results are presented as ng/mL.

Measurement of interleukin-10

- Plasma levels of IL-10 were determined using a Human IL-10 ELISA Kit (E-EL-H6154, Elabscience, Houston, TX, USA). Results are presented as pg/mL.

Measurement of CD163

- A Human CD163 SimpleStep ELISA (ab274394, Abcam, Cambridge, UK) was used to determine the concentration of CD163 in the stored plasma samples. The results are presented as pg/mL.

Measurement of CD206

- Levels of CD206 were measured by means of a Human Mannose Receptor ELISA (ab277420, Abcam). The results are presented as ng/mL.

Statistical Analysis

- The primary hypothesis was that that there was a significant difference in the plasma levels of soluble co-inhibitory immune checkpoints between BCC patients and healthy controls.
- Descriptive statistics were used to tabulate patient characteristics. The Mann Whitney U-test was used to compare levels of the various test biomarkers between BCC patients and healthy controls.
- The area under the ROC curve (AUC) was used as a measure of discriminatory ability for the biomarkers. The Youden index, a summary measure of the ROC curve, was used as an agnostic method for choosing an optimal cut-off value on the biomarker value to illustrate potential clinical usefulness.
- A correlation matrix report was used to identify correlations between variables (or subsets of variables) within the subset, using Spearman P-values to define significance.
- A p-value of less than .05 was considered statistically significant.
- NCSS 2021 software for Windows (USA) was used for statistical analyses.

Results

Table 1. Numbers of patients with: a) distinct clinical types of basal cell carcinoma (BCC); and b) basal cell carcinomas at distinct anatomical sites

Clinical subtype of BCC		Anatomical site	
Adenoid	(n=1)*	Cheek	(n=3)*,^
Basosquamous	(n=3)	Chest	(n=2)
Infiltrating	(n=22)	Ear	(n=4)
Infiltrating with squamous differentiation	(n=4)	Forearm	(n=4)
Keratotic	(n=1)	Forehead	(n=2)
Micronodular	(n=2)	Lower limb	(n=5)
Nodular	(n=5)	Neck	(n=2)
Pigmented	(n=1)^	Nose	(n=13)§
Superficial	(n=1)*	Shoulder	(n=1)
		Temple	(n=2)
		Upper anterior chest	(n=2)

**Numbers of patients are shown in parenthesis; *African patient; §Asian patient*

Table 2. Comparison of the systemic concentrations of soluble stimulatory, inhibitory and dual immune checkpoint molecules in patients with basal cell carcinoma and control participants.

Soluble immune checkpoints (pg/mL)	Patients with advanced basal cell carcinoma (n=40)	Control participants (n=20)	*p§*
CD27	3360 (2363 - 4970)	1410 (1259 - 2172)	0,0002
CD28	17047 (8487 - 30677)	11314 (7236 - 14883)	0,2523
CD40	1308 (968 - 1779)	1222 (769 - 1349)	0,4148
ICOS	15359 (7591 - 20308)	12902 (7980 - 15316)	0,3428
GITR	1217 (664 - 1795)	698 (228 - 1222)	0,0538
GITRL	2527 (1470 - 3599)	2107 (1784 - 2724)	0,3799
CD86	2215 (793 - 3292)	1636 (781 - 2144)	0,2427
CD80	1450 (863 - 2161)	1212 (781 - 1590)	0,3428
PD-1	10978 (5714 - 14351)	2524 (1832 - 3038)	0,0000
PD-L1	1740 (773 - 1980)	228 (139 - 274)	0,0000
PD-L2	14705 (13102 - 16375)	12008 (10670 - 14023)	0,0011
CTLA-4	744 (422 - 1129)	126 (56- 241)	0,0000
TIM-3	7519 (6619 - 8157)	2328 (1967 - 2667)	0,0000
LAG-3	388288 (243248 - 540480)	11106 (6595 - 15093)	0,0000
BTLA	12284 (8754 - 19151)	25439 (17274 – 32427)	0,0061
TLR-2	17696 (10473 - 24211)	15731 (12262 - 19913)	0,6437
HVEM	2052 (1894 - 2317)	1299 (1263 - 1458)	0,0000

**Results are expressed as the median values with 95% confidence intervals in parenthesis*

Table 3. Comparison of the systemic concentrations of arginase 1, RANTES, TGF-β1, FAP, IL-10, CD206, and CD163 in patients with basal cell carcinoma and control participants.

Biomarker	Patients with basal cell carcinoma (n=40)	Control participants (n=20)	*p§*
Arginase	25 (25 - 29)	25 (25 - 72)	0,2897
RANTES	131 (97 – 175)	91 (71 - 149)	0,2097
TGF-β1	7 (5 – 11)	5 (4 - 7)	0,1469
IL-10	0 (0 - 0)	0 (0 – 4)	0,1322
FAP	116 (94 - 130)	109 (71 - 127)	0,2425
CD206	227 (192 - 251)	188 (143-278)	0,502
CD163	218017 (194810 - 298215)	216818 (133047 - 272483)	0,2266

Results are expressed as median values with 95% confidence limits in parenthesis.
Results for arginase 1, RANTES, TGF-β1 and CD206 are presented as ng/mL while those for FAP, IL-10 and CD163 are presented as pg/mL.

Figures 1-5. (a) Comparison of plasma levels of inhibitory immune checkpoints between BCC patients and healthy controls; and (b) ROC curves of inhibitory immune checkpoints.

Figure 1a. TIM-3 levels of BCC patients vs healthy controls (p<0.00034)

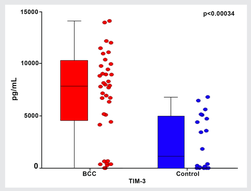

Figure 1b ROC curve of TIM-3 with AUC=0.85, confidence interval (95%): 0.72-0.92, p<0.0000).

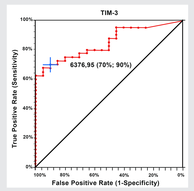

Figure 2a. LAG-3 levels of BCC patients vs healthy controls (p<0.00232)

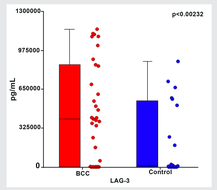

Figure 2b. ROC curve of LAG-3 with AUC=72, confidence interval (95%): 0.57-0.83, p<0.0004).

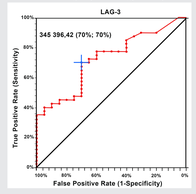

Figure 3a. PD-1 levels of BCC patients vs healthy controls (p<0.00274)

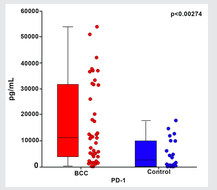

Figure 3b. ROC curve of PD-1 with AUC=0.75, confidence interval (95%): 0.59-0.85, p<0.0001).

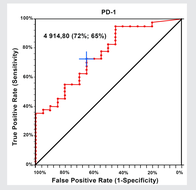

Figure 4a. CTLA-4 levels of BCC patients vs healthy controls (p<0.003)

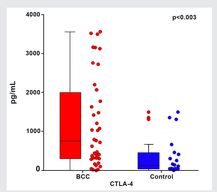

Figure 4b. ROC curve of CTLA-4 with AUC=0.76, confidence interval (95%): 0.60-0.86, p<0.0000).

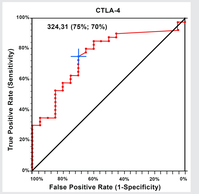

Figure 5a. PD-L1 levels of BCC patients vs healthy controls (p<0.02191)

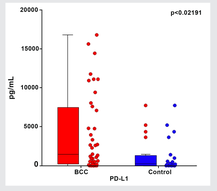

Figure 5b. ROC curve of PD-L1 with AUC=0.68, confidence interval (95%): 0.51-0.79, p<0.0052).

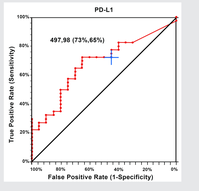

Figure 6. Correlations between FAP, RANTES, CD206, CD163, Arginase 1, and TGF-β1 with soluble immune checkpoint molecules

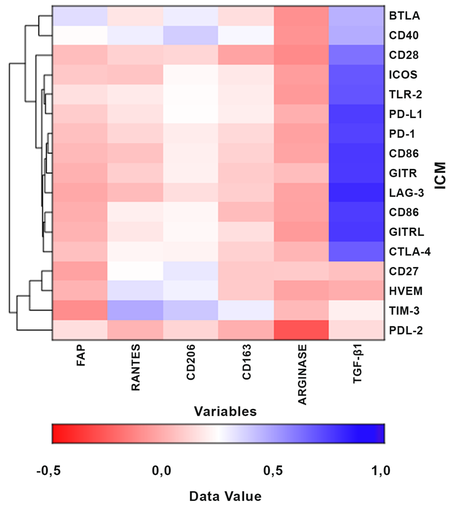

Figure 7. Associations of the soluble co-inhibitory immune checkpoints, LAG-3, PD-1 and PD-L1, CTLA-4 with TGF-β1.

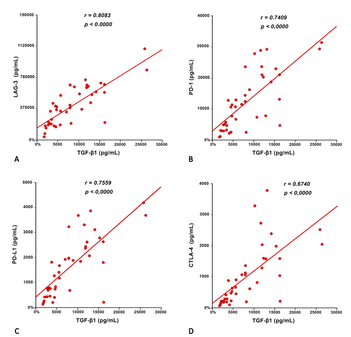

Figure 8. Associations of the soluble co-stimulatory immune checkpoints, CD80, CD86, GITR, GITRL, CD28, and ICOS, with TGF-β1.

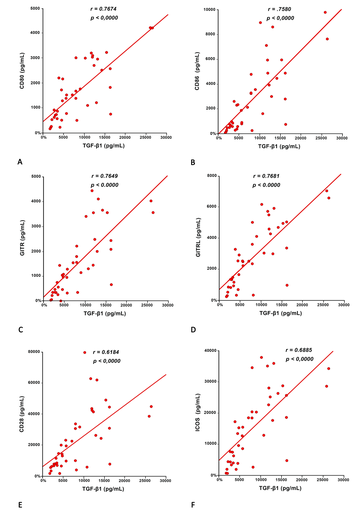

Figure 9. Association of the dual-active soluble immune checkpoint, TLR-2, with TGF-β1.

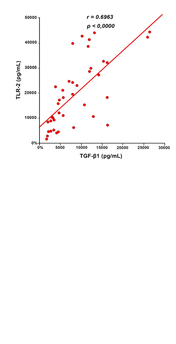

Conclusions

- High plasma levels of co-inhibitory sICPs, and a positive correlation with TGF-β1, were detected in BCC patients.
- These features are indicative of significant pro-tumorigenic immunosuppression.
- The role of co-inhibitory sICPs and plasma levels of TGF-β1 should therefore be investigated as possible predictors of response to treatment, as well as prognostic biomarkers in these patients.
- The therapeutic potential of combining anti-PD-1 antibodies with anti-TIM-3, anti-CTLA-4, anti-LAG-3, or with anti-TGF-β1 in advanced BCC patients is warranted.

References

1. Verkouteren, J.A.C.; Ramdas, K.H.R.;Wakkee, M.; Nijsten, T Epidemiology of basal cell carcinoma: scholarly review. Br J Dermatol. 2017 Aug;177(2):359-372. doi: 10.1111/bjd.15321. Epub 2017 Feb 20. PMID: 28220485
2. Seidi-Phillips M, Frischtut N, Hollweger N, Schmuth M, Nguyen VA. Known and new facts on basal cell carcinoma. J Dtsch Dermatol Ges. 2021 Jul;19(7):1021-1041. doi: 10.1111/ddg.14580. PMID: 34288482
3. Fania L, Didona D, Morese R, Campana I, Coco V, Di Pietro FR, Ricci F, Pallotta S, Candi E, Abeni D, Dellambra E. Basal Cell Carcinoma: From Pathophysiology to Novel Therapeutic Approaches. Biomedicines. 2020 Oct 23;8(11):449. doi: 10.3390/biomedicines8110449. PMID: 33113965
4. Kim DP, Kus KJB, Ruiz E. Basal Cell Carcinoma Review. Hematol Oncol Clin North Am. 2019 Feb;33(1):13-24. doi: 10.1016/j.hoc.2018.09.004. PMID: 30497670
5. Tanese K. Diagnosis and Management of Basal Cell Carcinoma. Curr Treat Options Oncol. 2019 Feb 11;20(2):13. doi: 10.1007/s11864-019-0610-0. PMID: 30741348 Review.
6. Hedgehog signaling promotes tumor-associated macrophage polarization to suppress intratumoral CD8+ T cell recruitment. J Clin Invest. 2019 Dec 2;129(12):5151-5162. doi: 10.1172/JCI129644. PMID: 31638600
7. Hinshaw DC, Hanna A, Lama-Sherpa T, Metge B, Kammerud SC, Benavides GA, Kumar A, Alsheikh HA, Mota M, Chen D, Ballinger SW, Rathmell JC, Ponnazhagan S, Darley-Usmar V, Samant RS, Shevde LA. Hedgehog Signaling Regulates Metabolism and Polarization of Mammary Tumor-Associated Macrophages. Cancer Res. 2021 Nov 1;81(21):5425-5437. doi: 10.1158/0008-5472.CAN-20-1723. Epub 2021 Jul 21. PMID: 34289986
8. Xie J. The hedgehog's trick for escaping immunosurveillance: The molecular mechanisms driving myeloid-derived suppressor cell recruitment in hedgehog signaling-dependent tumors. Oncoimmunology. 2014 Jun 5;3:e29180. doi: 10.4161/onci.29180. eCollection 2014. PMID: 25054089
9. Grund-Gröschke S, Stockmaier G, Aberger F. Hedgehog/GLI signaling in tumor immunity - new therapeutic opportunities and clinical implications. Cell Commun Signal. 2019 Dec 26;17(1):172. doi: 10.1186/s12964- 019-0459-7. PMID: 31878932
10. Valenti G, Quinn HM, Heynen GJJE, Lan L, Holland JD, Vogel R, Wulf-Goldenberg A, Birchmeier W. Cancer Stem Cells Regulate Cancer-Associated Fibroblasts via Activation of Hedgehog Signaling in Mammary Gland Tumors. Cancer Res. 2017 Apr 15;77(8):2134-2147. doi: 10.1158/0008-5472.CAN-15-3490. Epub 2017 Feb 15. PMID: 28202523
11. Omland SH, Nielsen PS, Gjerdrum LM, Gniadecki R. Immunosuppressive Environment in Basal Cell Carcinoma: The Role of Regulatory T Cells. Acta Derm Venereol. 2016 Nov 2;96(7):917-921. doi: 10.2340/00015555-2440. PMID: 27117439
12. Omland SH, Hamrouni A, Gniadecki R. High diversity of the T-cell receptor repertoire of tumor-infiltrating lymphocytes in basal cell carcinoma. Exp Dermatol. 2017 May;26(5):454-455. doi: 10.1111/exd.13240. Epub 2017 Jan 19. PMID: 27714856
13. Omland SH, Wettergren EE, Mollerup S, Asplund M, Mourier T, Hansen AJ, Gniadecki R. Cancer associated fibroblasts (CAFs) are activated in cutaneous basal cell carcinoma and in the peritumoural skin. BMC Cancer. 2017 Oct 7;17(1):675. doi: 10.1186/s12885-017-3663-9. PMID: 28987144
14. Omland SH. Local immune response in cutaneous basal cell carcinoma. Dan Med J. 2017 Oct;64(10):B5412. PMID: 28975891
15. Zhang Y, Zheng J. Functions of Immune Checkpoint Molecules Beyond Immune Evasion. Adv Exp Med Biol. 2020;1248:201-226. doi: 10.1007/978-981-15-3266-5_9. PMID: 32185712
16. Tu L, Guan R, Yang H, Zhou Y, Hong W, Ma L, Zhao G, Yu M. Assessment of the expression of the immune checkpoint molecules PD-1, CTLA4, TIM-3 and LAG-3 across different cancers in relation to treatment response, tumor-infiltrating immune cells and survival. Int J Cancer. 2020 Jul 15;147(2):423-439. doi: 10.1002/ijc.32785. Epub 2019 Dec 2. PMID: 31721169
17. Gu D, Ao X, Yang Y, Chen Z, Xu X. Soluble immune checkpoints in cancer: production, function and biological significance. J Immunother Cancer. 2018 Nov 27;6(1):132. doi: 10.1186/s40425-018-0449-0. PMID: 30482248
18. Chakrabarti R, Kapse B, Mukherjee G. Soluble immune checkpoint molecules: Serum markers for cancer diagnosis and prognosis. Cancer Rep (Hoboken). 2019 Aug;2(4):e1160. doi: 10.1002/cnr2.1160. Epub 2019 Feb 7.PMID: 32721130